

Article

# Reconstituted Keratin Biomaterial with Enhanced Ductility

Halleh Atri <sup>\*</sup>, Elham Bidram and David E. Dunstan

Received: 10 August 2015 ; Accepted: 20 October 2015 ; Published: 5 November 2015

Academic Editor: Carsten Werner

Department of Chemical and Biomolecular Engineering, University of Melbourne, Parkville, VIC 3010, Australia; elhamb@student.unimelb.edu.au (E.B.); davide@unimelb.edu.au (D.E.D.)

\* Correspondence: h.atri@student.unimelb.edu.au; Tel.: +61-3-8344-4888 (ext. 44888)

**Abstract:** Nowadays the waste from protein fibres represents an important renewable source for a new generation of biomaterials and promising competitors for carbohydrate based biomaterials. Regenerated keratin biomaterials are biodegradable *in vivo* and *in vitro*, biocompatible, and support cell attachment and proliferation; however, their major drawback has been their weak mechanical properties such as ductility. The following study was conducted in an attempt to improve the ductility of reconstituted keratin films obtained from Australian merino wool fibres. Keratin was extracted from wool fibres according to an established protocol proposed by Yamauchi, and then dialyzed and desaltsed by multiple diafiltration wash cycles. The resulting keratin film was transparent, biodegradable, and, opposite to its predecessors, mechanically durable, possessing a Young modulus about 12.5 MPa with 35% extensibility. The polypeptide chains were found to rearrange themselves in the  $\beta$ -sheet state in this keratin film, which was shown to be semi-crystalline. This film, unlike its predecessors, did not support human cell proliferation. These properties of the diafiltered keratin film have led us to think that diafiltration resulted in producing a totally new keratin film, which is envisaged to find applications in various areas.

**Keywords:** recycling; keratin; biodegradability; mechanical properties; cell attachment

---

## 1. Introduction

The demand for eco-friendly products has increased significantly in different sectors in recent years [1–3]. In the textile sector, the existing concerns for the environment—as well as rising oil prices—are driving research to focus on environmental friendly fibres; for instance, 38 million tonnes of synthetic fibres are produced annually in the world (mainly polyester, nylon and olefin fibre), and they are not biodegradable posing a threat to the environment [3].

Recently, proteins have emerged as potentially suitable candidates for a new generation of biomaterials due to their inherent properties such as biodegradability, natural abundance and durability [3]. Some of these proteins—which have been used to develop new biomaterials—are collagen [4], albumin [5], gelatine [6,7], fibroin [8,9], and keratin [10–12]. Keratin, which is a fibrous protein, can be found in wool, feather and hair fibres. Keratin fibres and their waste are an important and abundant renewable source of biopolymers [13–17]. It is estimated that about one million tons of hair and four million tons of feathers are produced every year worldwide [18,19] (according to the Indian ministry of textiles, raw wool consumption is estimated to reach 260.8 million kg by 2020 [20]), and the disposal of their wastes raises both environmental and economic issues [18–22]; for instance, an extensive amount of landfill is needed for their burial while their decomposition is very slow due to the large number of S–S linkages. Recycling the protein of these fibres will resolve the aforementioned problems; moreover, biomaterials derived from hard  $\alpha$ -keratin fibres are promising competitors for other environmental friendly materials with high added value [3].

Hard  $\alpha$ -keratin fibres—such as wool, hair and feather—show a fibrillar organization from micrometre to nanometre scale, and they consist of parallel microfibrils or IFs (7–8 nm in diameter) and an amorphous matrix. Keratin fibrils are made of low sulphur proteins belonging to the intermediate filament (IF) family. IFs are the third major cytoskeleton entity comprising of 10 nm wide filaments; the common property of IFs is their tripartite domain structure, which consists of a non-helical head (N-terminal) and a tail (C-terminal) with a central  $\alpha$ -helical domain [23–25]. Intermediate filament-associated proteins (IFAP)—which form the keratin matrix—include sulphur-rich (HS) proteins, proteins with an ultrahigh content of sulphur (UHS), and the glycine-tyrosine-rich (HGT) proteins.

Keratin from hair and wool fibres can be recovered and transformed into biomaterials with distinct properties. In summary, keratin extraction from hard  $\alpha$ -keratin fibres is only possible when the disulphide bonds are reduced, by thiols such as thioglycolic acid, or oxidized, by peracetic or performic acid [26,27]. In addition to a reducing agent, a protein-denaturing agent such as urea should be used to break the hydrogen bonds and achieve an extraction yield of about 50% to 70% wt. Earlier research has shown that keratin biomaterials are biodegradable *in vivo* and *in vitro*, biocompatible, commercially abundant and of consistent quality [10]. These new materials can find applications in textile and non-textile areas, compostable packaging, disposables, agricultural films, membranes and coatings [27,28]. In recent years, regenerated wool keratin has been utilized as a substrate or scaffold in cell cultivation and tissue engineering. It has been reported that keratin coated plates and sponges improve fibroblast cell attachment and proliferation [29–31]. Regenerated keratin films from human hair have been recently shown to be promising candidates for ocular surface reconstruction [12]. Keratin nano fibres were also produced from recycled wool fibres and found applications in membrane technology and medical science [11,32,33].

Despite the advantages of producing regenerated keratin materials, keratin biomaterials have poor mechanical properties—elongation at break and ultimate strength—and thus they have to be employed in combination with either synthetic or natural polymers such as PEO (polyethylene oxide), chitosan, collagen and silk fibroin. It is hypothesized that the excessive number of cysteine crosslinks (S–S linkages) in keratin films is the main reason for their brittleness [34,35].

In the following study, a mechanically robust keratin biomaterial was produced by diafiltration of keratin extracted from Australian merino wool fibres. The keratin extract and the obtained keratin film (before and after diafiltration) were characterised by Lowry and Ellman assays, SDS-PAGE (sodium dodecyl sulphate polyacrylamide gel electrophoresis), DLS (dynamic light scattering), FTIR (Fourier transform infrared spectroscopy) and XRD (X-ray powder diffraction). Instron tensile tester determined the mechanical properties of the product such as its Young's modulus, extensibility or elongation at break, and strength. ESEM(environmental scanning electron microscopy) imaged the keratin films, and then the films were used in human cell culture experiments to study their toxicity as well as their effect on cell growth and proliferation.

## 2. Results and Discussion

### 2.1. Keratin Extraction, Purification and Characterization

The total weight of protein extracted from wool fibres following to dialysis and diafiltration was determined to be 30 mg for 1 mL of solution. The concentration of keratin extract was estimated to be about 2 mg/mL, based on the bovine serum albumin (BSA) standard curve with Lowry assay which estimated the concentration of protein based on tyrosine amino acids present in the solution. Although dialysis with cellulose tubing has been recommended as an efficient purification method for keratin [29–35], this study revealed the necessity of further filtration of the sample with double distilled water as many times as it was desired to remove all impurities including the salts used for keratin extraction—14 cycles of diafiltration was performed in this study; this number depends on the amount of salts and quality of the membrane. The conductivity of keratin

extract after each cycle was measured by conductance metre to confirm the efficiency of the filtration process and removal of the salts; the conductivity of the keratin extract reduced during dialysis from 700–800  $\mu\text{S}/\text{cm}$  to 400–500  $\mu\text{S}/\text{cm}$  for keratin extract before and after dialysis respectively. This value declined to 80–120  $\mu\text{S}/\text{cm}$  after 14 cycles of diafiltration of the extract. The reduction of conductivity during dialysis and diafiltration indicated the removal of salt ions and charged amino acids from keratin extract. The keratin extract before dialysis had a pH of about 8, and it was found that if the pH dropped below 6.2, keratin would precipitate out of the solution resulting in a cloudy solution (keratin isoelectric point is 4.5–6), and thus the pH of the solution was adjusted to be always above that value with sodium hydroxide during diafiltration. The efficiency of removing reducing agent from the extract during dialysis and diafiltration was monitored by Ellman assay, which revealed a reduction in the concentration of free thiol groups in the soluble keratin after filtration. The molecular weight of all constituents of the keratin extract from every filtration step was determined with SDS-PAGE (Figure 1).

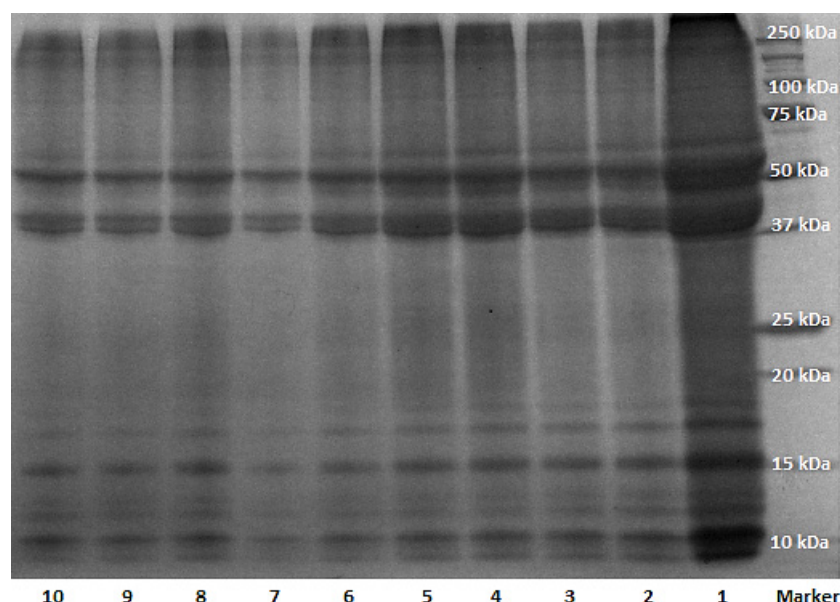


**Figure 1.** SDS-PAGE (sodium dodecyl sulphate polyacrylamide gel electrophoresis) of keratin extract from different steps of dialysis and diafiltration; samples 1–4: D0–D3 (D = dialyzed and the number corresponds to days); samples 5–10: DF1, DF3, DF5, DF8, DF10, DF14 (DF = dialyzed and diafiltered and the number corresponds to cycles).

In Figure 1, all 10 samples from various filtration steps displayed the characteristic bands of keratin IFs and the matrix component [34]. The SDS-PAGE of keratin had two major bands around 37 and 50 kDa, which have been attributed to the keratin IFs; there were also multiple low molecular weight bands (10–20 kDa) attributing to keratin matrix proteins [35]. The average protein content attributing to keratin IFs was determined by densitometry and shown in Figure 2. The protein content in the IFs constituent of keratin extract (37 and 50 kDa) decreased significantly during dialysis, and then it reached an almost constant value during diafiltration.

The average values for diameter and polydispersity of the keratin extract constituents were approximated to be 100 nm and 0.2, respectively, indicating the monodisperse medium of keratin extract (see Figure 3). Although these values decreased significantly after dialysis, diafiltration did not affect them.

It is important to note that although the diameter, polydispersity, and the amount of protein in the solution reached constant values after five cycles of diafiltration, the conductivity of the keratin

extract was still reducing; therefore, more cycles of diafiltration were performed until a constant value was obtained—about 80  $\mu\text{S}/\text{cm}$ .

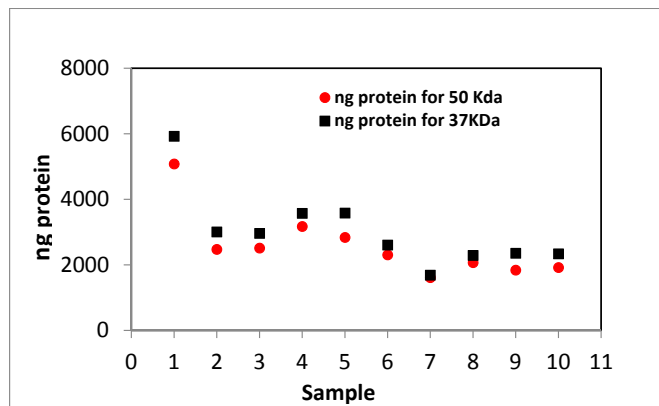


**Figure 2.** Densitometry results for the amount of protein obtained for 50 kDa band and the 37 kDa in different samples from SDS-PAGE. Samples 1–4: D0–D3 (D = dialyzed and the number corresponds to days); samples 5–10: DF1, DF3, DF5, DF8, DF10, DF14 (DF = dialyzed and diafiltered and the number corresponds to cycles).

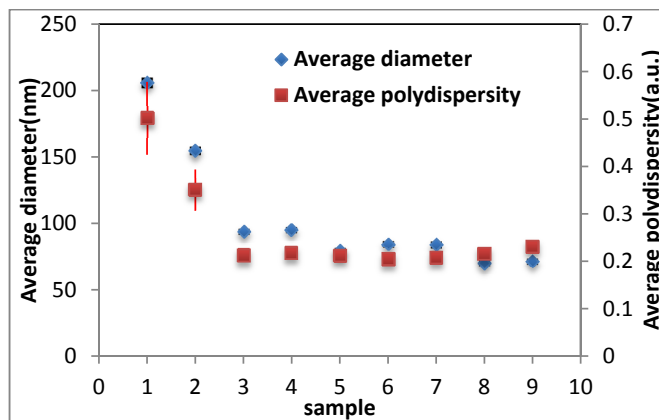


**Figure 3.** Average diameter and polydispersity of keratin extract constituents from different filtration steps determined by DLS from three repeats. Samples 0–3: D0–D3 (D = dialyzed and the number corresponds to days); samples 4–9: DF1, DF3, DF5, DF8, DF10, DF14 (DF = dialyzed and diafiltered and the number corresponds to cycles). The data for sample D0 (keratin extract before dialysis) was out of range and not shown.

## 2.2. Keratin Film Characterization

The extract from before (sample 4) and after diafiltration (sample 10) was air dried in a regular glass petri dish to obtain transparent keratin films that were about 1 mm thick. These films were then characterized with multiple techniques such as X-ray powder diffraction, FTIR and scanning electron microscopy. In Figure 4, the FTIR and XRD spectra of keratin films, which were obtained either by dialysis or diafiltration, were shown. According to FTIR and XRD spectra, the protein chains re-arranged themselves in the  $\beta$ -sheet state in both films, but the film obtained after diafiltration had more  $\beta$ -sheet content. The peak at  $2\theta = 20^\circ$  ( $q: 13.51 \text{ nm}^{-1}$ ) in the XRD plot was attributed to the  $\beta$ -sheet characteristic peak that shows the distance between  $\beta$ -strands, and it is about 0.465 nm; this peak was sharp and intense in the diafiltered keratin film. In the previous studies, no crystalline reflection was detected for keratin film, which suggested the lack of any particular arrangement of

keratin chains in the film [12], but the existing peak in Figure 4a inferred the existence of a crystalline organization in the diafiltered keratin film. FTIR spectra of both dialyzed and diafiltered keratin films were shown in Figure 4b; both spectra revealed similar peaks with different intensities. They both contained  $\beta$ -sheet characteristic bands for amide I ( $1630\text{ cm}^{-1}$ ) and amide II ( $1230\text{ cm}^{-1}$ ). There was a band appearing in the absorption plots of diafiltered and dialyzed keratin films at  $1277\text{ cm}^{-1}$  attributed to the amide III in the  $\beta$ -sheet structure; this band was more intense in the absorption plot of diafiltered keratin film. The band at  $1042\text{ cm}^{-1}$  has been assigned to a symmetric S=O stretching vibration of sulphonate groups of cysteic acid residues [35].

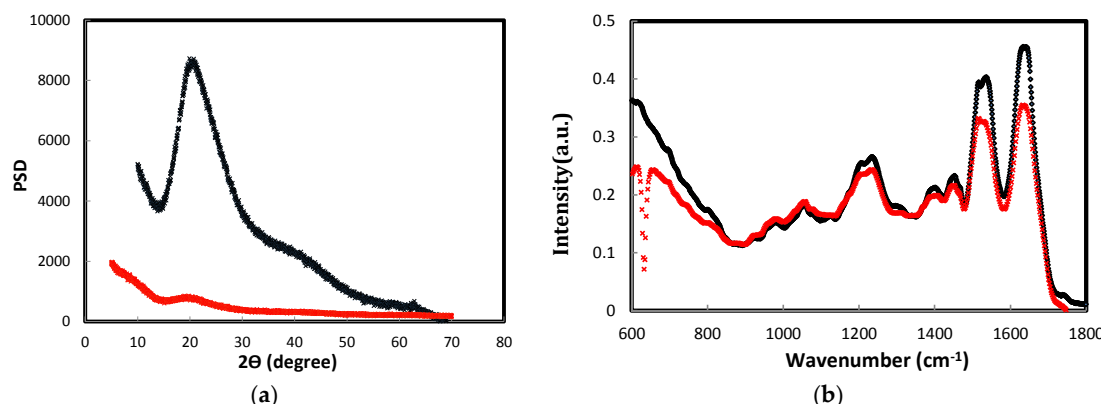


**Figure 4.** (a) X-ray powder diffraction of keratin films; PSD stands for power spectral density of any signal; (b) FTIR (Fourier transform infrared spectroscopy) of keratin films. The black spectrum was obtained from dialyzed and diafiltrated keratin film after 14 cycles of diafiltration; the red plot was obtained from dialyzed keratin film after three days of dialysis.

The diafiltrated keratin film was then stained with 1% Congo red which was dissolved in 10% ethanol, and then the stained film was left to be air dried and observed between crossed-polarizers. Congo red is a diazo dye first synthesized in 1883, and it shines not red but a greenish hue termed “apple-green birefringence” under polarized light upon interacting with amyloid fibrils—which are made of  $\beta$ -sheets [36]. In Figure 5, the green colour appeared in the Congo red stained diafiltrated keratin film—against dark back ground—was an evidence of the presence of  $\beta$ -sheet structures in the diafiltrated keratin film. The appearance of red colour in the image might be due to the presence of water molecules in the film meaning the bottom layers were not as dry as the surface of the film. It is important to note that the keratin film was transparent, and therefore the light could pass through the film and reveal the internal layers.

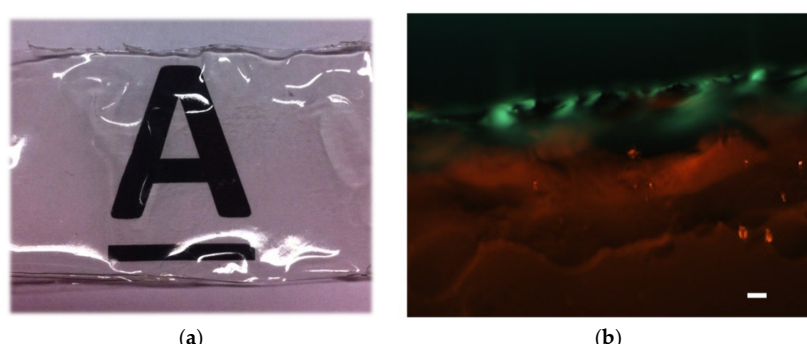


**Figure 5.** (a) Transparent keratin film obtained by 14 cycles of diafiltration (the image was taken by a camera); (b) Congo red stained keratin film (obtained by 14 cycles of diafiltration) between crossed polarizers, which shows apple-green birefringence. Scale bar:  $5\text{ }\mu\text{m}$ .

The transparent keratin film—which was obtained after dialysis and desalting by diafiltration—is shown in Figure 5a, and the SEM (scanning electron microscopy) images of this film were shown in Figure 6. From these images, the obtained keratin film after multiple diafiltration steps was non-porous (see SEM images), and it had a very smooth surface. In contrast to this film, the film that was obtained only by dialysis was porous, and the pores were big and entangled enough to be detected by light microscopy, see Figure 6a.

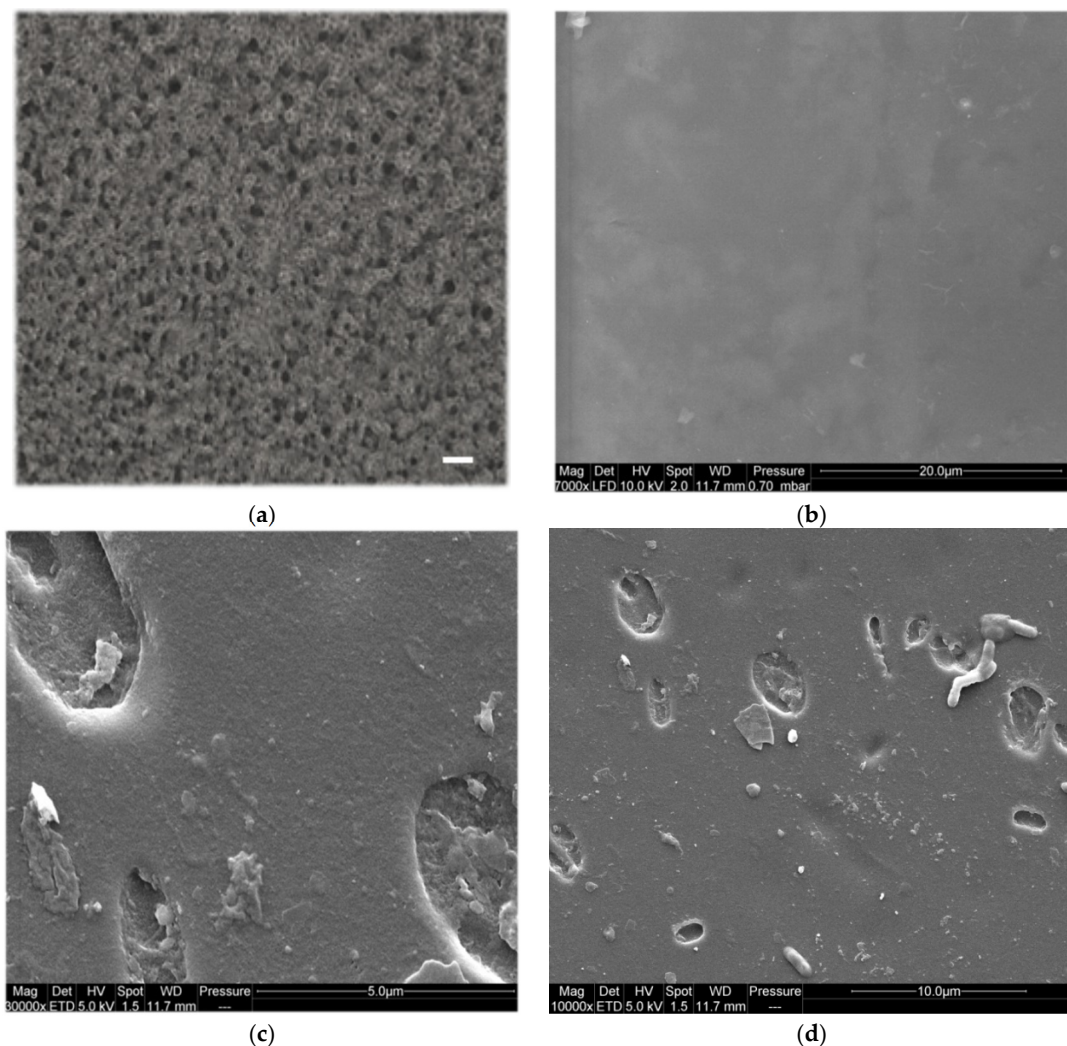


**Figure 6.** (a) Light microscopy image of the keratin film obtained after three days of dialysis, scale bar: 5  $\mu\text{m}$ ; (b–d) ESEM (sodium dodecyl sulphate polyacrylamide gel electrophoresis) images of keratin film obtained after 14 cycles of diafiltration imaged under low vacuum conditions; (b) Freshly made keratin films; and (c–d) keratin films soaked in water for two months showing bacterial growth and biodegradability.

SEM images from diafiltered keratin film (Figure 6b–d) revealed the strikingly smooth surface of keratin films. No porosity was detected in these films for high as well as low magnifications (7000–50,000 $\times$ ). The biodegradability of keratin films was confirmed by the observation of bacterial growth on the surface of the films and also by trypsin digestion in less than 10 h.

## 2.2.1. Mechanical Properties of the Keratin Film

The fragility of keratin film has been reported frequently in the literature [12,13,34]. In order to circumvent the brittleness of keratin film, it is often necessary to add additives such as glycerol,

chitosan or other polymers such as polyethylene oxide to keratin solution [10,37,38]. Mechanical properties of keratin film from previous studies have been summarized in Table 1; it is often reported that pure keratin film is fragile and difficult to handle.

**Table 1.** Mechanical properties of keratin film which have been reported in different studies.

Keratin Film	Ultimate Strength (MPa)	Young Modulus (MPa)	Elongation (%)
Compression molded [35]	20–27	710–1218	1–4
Non-treated keratin film [38]	-	-	-
Chitosan/keratin film [38]	9–14	92–111	18–31
Chitosan/Glycerol/keratin [38]	27–34	160–310	4–5
Dry keratin film for ocular surface regeneration [12]	20	300	-
Dry Keratin film from this study	20–30	12–15	30–40

The keratin film that was obtained in this study after the dialysis was very fragile, difficult to handle, and it was not possible to measure its mechanical properties. In contrast to this film, the film in which keratin was desalinated and diafiltered was much stronger and easier to handle. The mechanical properties of this film were measured and shown in Figure 7; this film had mechanical properties of the order of MPa (the keratin films were cut to rectangles of similar sizes for this measurement). The Young's modulus ( $E$ ) was obtained from the following formulas:

$$\frac{\sigma}{\epsilon} = E \text{ Hooke's Law} \quad (1)$$

$$\frac{F}{A} = \sigma F : \text{load (N)} ; A : \text{area (m}^2\text{)} ; \sigma : \text{stress (Pa)} \quad (2)$$

$$\frac{\Delta L}{L} = \epsilon \Delta L : \text{elongation}; L : \text{initial length}; \epsilon : \text{strain} \quad (3)$$

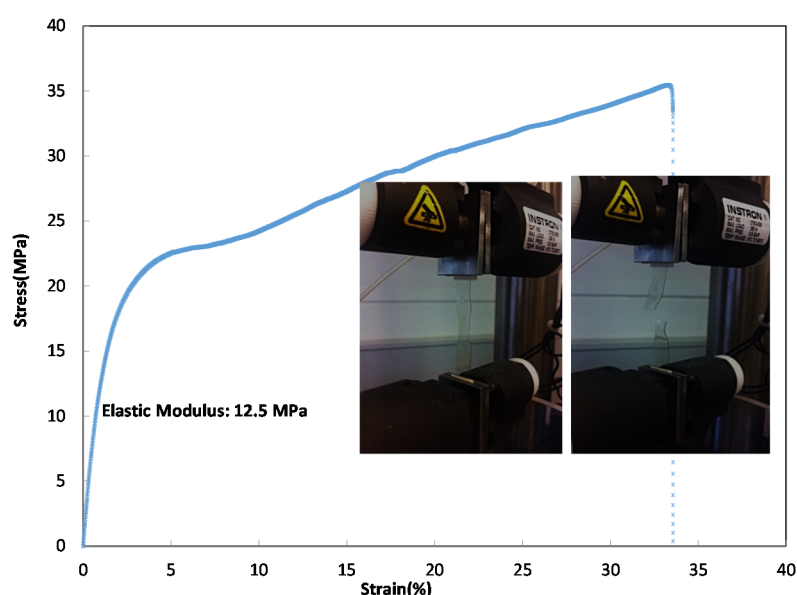


**Figure 7.** Stress–strain curve of dialyzed and diafiltered keratin film.

### 2.2.2. Cell Culture Experiments

The dialyzed and diafiltered keratin films were then used in cell culture experiments. Two different cell lines (fibroblast 3T3 and MDA-BA-231 (mitochondria of highly metastatic breast cancer cells)) were cultured on the keratin-coated plates and the cell growth, morphology and proliferation were monitored by light microscopy. The toxicity of the films was then studied by WST (water-soluble tetrazolium salts) cytotoxicity assay. Figure 8a,d show the fibroblast and MDA breast cancer cells, which grew well on the uncoated dish. For dialyzed keratin coated dishes (Figure 8b,e), the cells also grew and spread well showing an elongated morphology, but the cells on the diafiltered keratin film had a very different morphology (Figure 8c,f). They were round, and they did not spread on the plate in comparison with the uncoated dish. The result for WST assay was shown in Figure 9 in which some toxicity was detected for diafiltered keratin film.

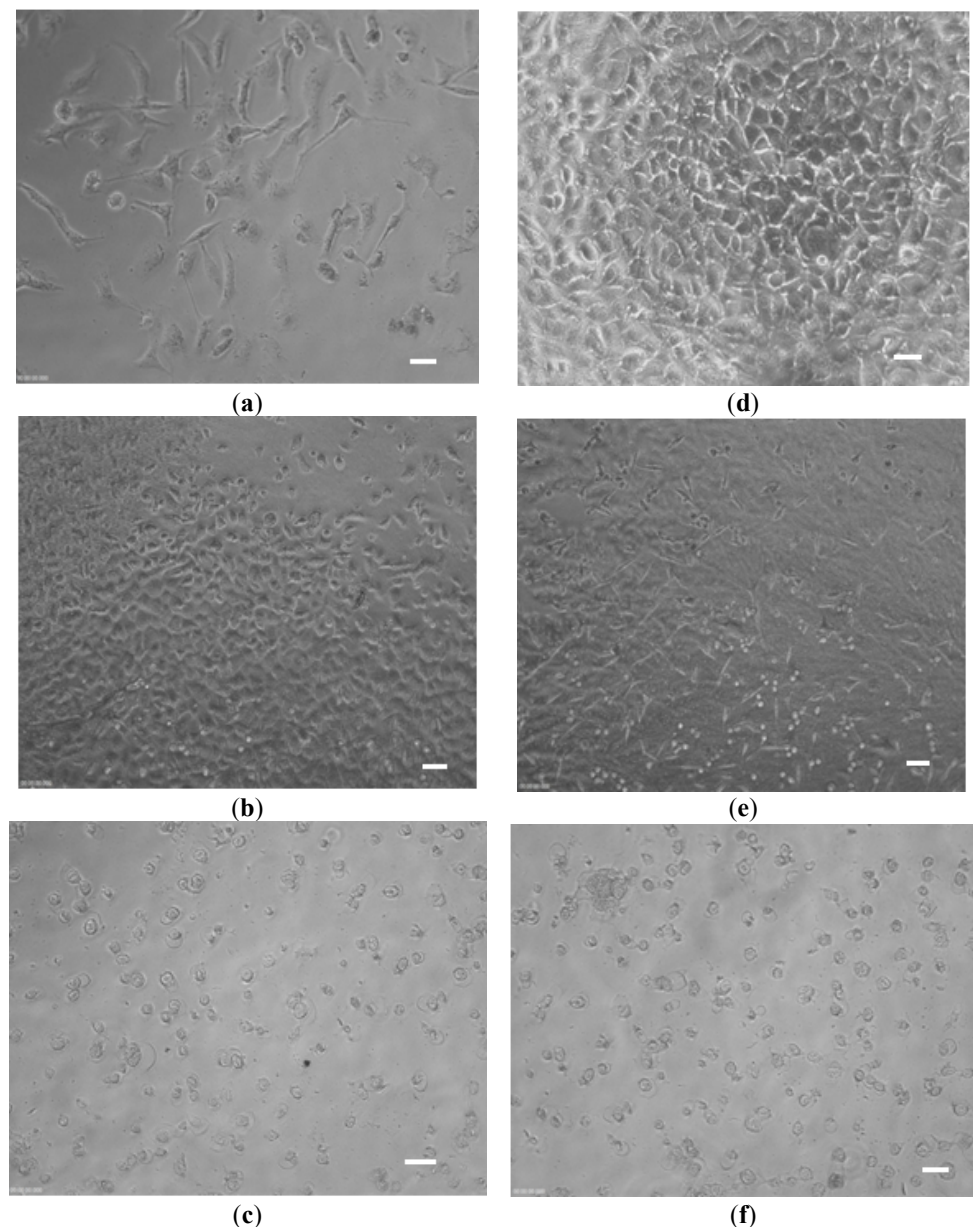


**Figure 8.** Fibroblast (a–c) and MDA breast cancer cells (d–f) were cultured on the plates after 24 h incubation; (a,d) uncoated, (b,e) dialyzed keratin coated, and (c,f) diafiltered keratin coated. Scale bar: 5  $\mu$ m.

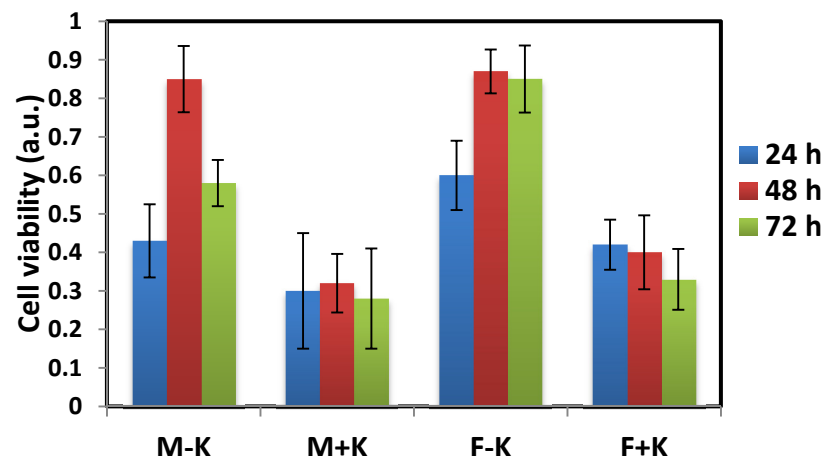


**Figure 9.** Cell viability on the keratin-coated plates was determined by WST assay after 24, 48 and 72 h incubation. M stands for MDA breast cancer cells, K stands for keratin and F is for fibroblast cells. Error bars were obtained from three independent measurements.

### 3. Experimental Section

Soluble keratin was obtained from merino wool fibres (provided in already cleaned wool tops) by Yamauchi method [34,35]. For extraction, certain amount of fibre was treated with 8 M of urea 1.66 M of  $\beta$ -mercapto ethanol, and 0.26 M of sodium dodecyl sulphate (SDS). The reaction was carried out at 50 °C for 16 h. Keratin extract was subsequently filtered through a 120  $\mu\text{m}$  stainless steel mesh and then centrifuged at 9000 rcf for 20 min to remove insoluble component. The centrifuged sample was then dialyzed with 6–8 kDa cellulose dialysis tubing (Spectrum Laboratories Inc. regenerated cellulose dialysis membrane) in 5 L of double distilled water for three days, providing the water was changed every day (dialyzed keratin sample). All chemicals were of standard grade and provided by Sigma. The resulting dialyzed extract was further purified by membrane filtration (diafiltration) in which 10 kDa cassette membrane was used to remove the remaining salt and also small molecular weight protein chains; the purest keratin sample was desalting in 14 wash cycles (diafiltered keratin sample). Salt molecules with small molecular weights passed the membrane as permeate, and retentate was collected as a purified keratin sample. In order to perform the filtration effectively, a peristaltic pump was employed to obtain a constant flow rate across the membrane. The system operated in dead-end mode in which the flow of the feed solution was perpendicular to the membrane surface. For keratin diafiltration, a 10 kDa Pelicon RXL cassette made of polyethersulfone (manufacturer) was used while maintaining 40  $\text{mL} \cdot \text{min}^{-1}$  flow rate across the membrane. Two main products were obtained and characterized from this extraction: (1) dialyzed keratin and (2) dialyzed and diafiltered keratin extract, these two products were then air-dried to obtain a solid film. This process was shown in Figure 10.

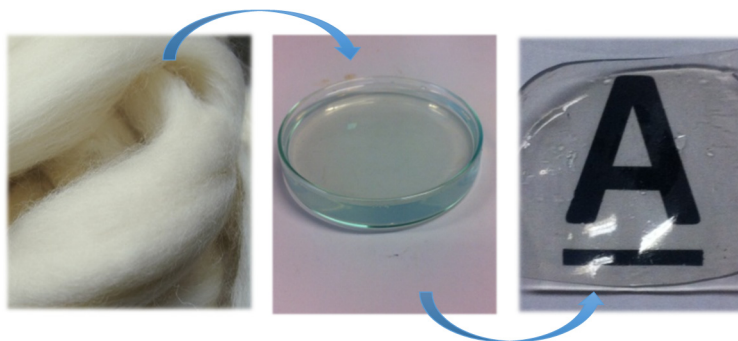


**Figure 10.** This schematic shows the process in which keratin film has been produced, starting from wool fibres, and the final product, which is the transparent and robust keratin film. Middle image shows transparent keratin extract.

Lowry and Ellman assay were carried out on keratin extract according to their established methods [39,40]. All the required chemicals for these assays were provided by Sigma.

SDS-PAGE was performed after each extraction, dialysis and diafiltration to assure that the product of interest has been produced. The experiment was performed according to Laemmli method [41]. For sample preparation, 10  $\mu$ L of denaturation buffer (denaturation buffer consists of 10 mM Tris HCl and 1 mM EDTA, pH= 8) was added to 10  $\mu$ L of keratin extract. Then 18  $\mu$ L of the loading buffer (Laemmli buffer) was added to the extract with 2  $\mu$ L  $\beta$ -mercapto ethanol (5%), reaching the final volume of about 40  $\mu$ L. The samples were then boiled for 5 min to be denatured completely, and then 10  $\mu$ L of each sample was loaded in the polyacrylamide gel. The gel was run at 100 V, 3 A and 300 W for 2 h, and then it was taken out, rinsed with millipore water 3 times, and then stained with Coomassie brilliant blue (Bio-safe Coomassie G-250 stain with 5% phosphoric acid) for 1 h. De-staining was carried out in millipore water for 1 h to prepare the gel for further analysis and imaging. Imaging was performed on the Bio-Rad molecular imager Gel Doc XRT (Bio-Rad, Melbourne, Australia) equipped with image lab software for data analysis and densitometry.

The average diameter of the extract constituents and its polydispersity were estimated with dynamic light scattering (Zeta sizer Nano ZS Malvern, Worcestershire, UK). The presented data was an average for 3 readings.

FTIR was carried out on Varian FTS 7000 (Agilent, Santa Clara, CA, USA) to determine the secondary structure of protein (keratin chains) in the dialyzed and diafiltered keratin films. Keratin films were minced in to small pieces before the measurement. One hundred scans were taken in the range 400–4000  $\text{cm}^{-1}$  with a resolution of 4  $\text{cm}^{-1}$ .

The X-ray diffraction pattern of minced keratin films were obtained using a D/max-2550 PC X-ray diffractometre (Rigaku Corporation, Tokyo, Japan) which used Cu K target at 40 kV, 300 mA and  $\lambda = 1.542 \text{ \AA}$ . The measurements were performed from 3 to 70° with a step size of 0.041°.

Polarization microscopy and light microscopy were performed on Olympus IX50 (Tokyo, Japan) to observe the structure of both dialyzed and diafiltered keratin films.

In order to determine the mechanical properties of keratin films, a set of tensile tests were carried out with Instron 5848 micro tester (Instron, Norwood, MA, USA). 50 kN load cell was chosen for conducting these tensile tests. The films (1 mm thick) were cut in to rectangles of similar sizes (30 mm  $\times$  7 mm) for these measurements (10 samples were used), and they were stretched at 10  $\text{mm} \cdot \text{min}^{-1}$  at 25 °C and 45% RH%. The samples were secured in the clamps to avoid any slippage. The reported data was from samples, which broke from the middle zones and not close to the clamping zones.

Scanning electron microscopy (SEM) was performed on FEI Quanta FEG 200 ESEM, made in Brno, Czech Republic; keratin films—which were obtained after 14 cycles of diafiltration—were used for SEM imaging.

For cell experiments, T3T fibroblasts and MDA-BA-231 breast cancer cells were grown to confluence in T225 flasks in DMEM medium (supplemented with 10% FBS, 1% L-glutamine, and 1% Pen-Strep) at 37 °C in 5% CO<sub>2</sub> atmosphere with 95%–100% humidity. On the day of the experiment, cells were trypsinized off the T-flask using 0.05% Trypsin-EDTA, counted manually using trypan blue as live/dead stain, diluted with fresh medium to reach a seeding density of 0.5 × 10<sup>5</sup> cells/mL and then plated onto 96 well plates (NUNC) wells covered by keratin film (10 µL/well) at a seeding volume of 100 µL/well, whereby some wells were left uncovered to serve as cell-negative controls. Plates were then placed in incubator for 24 and 48 h incubation. After this time, cells were monitored under the microscope to see any changes in their appearance as well as cell proliferation/toxicity assay (WST, CCK-8 cell counting kit from Sigma) to see the effect of keratin film on cell viability, which was added to the plates. Plates were gently rocked to facilitate mixing and then returned to the incubator for 1–4 h. In periodic intervals the UV/V is absorbance of the plates was read at 450 nm (absorbance of product produced by metabolically active cells upon addition of the WST reagent). Usually sufficient color was developed after approximately 2 h incubation. Absorbance values at 450 nm were corrected for background absorbance (690 nm) and absorbance of the medium alone (cell-blank controls), and then normalised to the growth control.

#### 4. Conclusions

In this study, keratin extract was obtained in a chemical reaction from wool fibres, and subsequently it was purified by conventional dialysis followed by multiple diafiltration against a 10 kDa membrane with double distilled water. During the diafiltration, the conductivity of the extract was monitored and shown to decline due to the removal of salts and charged amino acids in low molecular weight protein fragments. SDS-PAGE from keratin extract (before and after dialysis and diafiltration) confirmed the associated molecular weight bands for IFs and matrix components of keratin, and densitometry did not show a significant change in the concentration of these components due to diafiltration; however, SDS-PAGE image revealed less protein fragments between 15 and 37 kDa molecular weights bands for diafiltered samples. Moreover, DLS did not show much change in the diameter and polydispersity of keratin extract from different cycles of diafiltration. Therefore, these results suggested that diafiltration did not change the components of keratin extract, and it only assisted with removing the remaining salts in keratin samples. Dialyzed and diafiltered keratin samples were then air dried to obtain keratin films; the films were characterized by FTIR and XRD. FTIR showed that the polypeptide chains in both films were re-arranged to the β-sheet state, but the concentration of β-sheets was higher in the diafiltered keratin sample. An intense crystalline peak was detected in the XRD plot of diafiltered keratin film revealing the existence of crystallites in this film; this peak was associated with the distance between polypeptide chains in the β-sheet structures. The same peak appeared in the XRD plot of dialyzed keratin film, but the intensity of the peak was not comparable with the diafiltered one. Congo red stained diafiltered keratin film demonstrated apple-green birefringence when observed between crossed polarizers, and this was another evidence for the existence of β-sheets in the film. The porous structure of dialyzed keratin film was confirmed by light microscopy; this film was fragile, and it could not be employed by itself. On the other hand, the diafiltered keratin film—obtained in this study—was transparent, robust, and it had a very smooth surface with no porosity. Trypsin digestion and bacterial growth on the surface of this film confirmed its biodegradability. Diafiltration has significantly improved the mechanical properties of keratin film with Young's modulus of about 13 MPa and 40% extensibility. Based on these results, although the components of keratin in both dialyzed and diafiltered keratin samples were the same, the presence of salt crystals and disordered polypeptide chains in the dialyzed keratin film should contribute to the poor ductility of the film. As for the semi-crystalline structure of the diafiltered keratin film and its effect on the mechanical properties, although higher crystallinity should result in higher modulus and fragility, the removal of the salts by diafiltration should result in less fragility and more extensibility. This study showed that the latter had a more prominent

effect on the mechanical properties of these films, and diafiltered keratin films possessed higher elongation at break and lower modulus. Diafiltration might also remove some polar amino acids such as tyrosine that were present in the keratin matrix; removing these amino acids might affect the swelling, water absorption and consequently mechanical properties of the keratin films. Dialyzed keratin film absorbed and held water equal to three times as much as its weight, and it was a hydrogel, while the diafiltered keratin film absorbed water equal to about 50% of its weight, it was dimensionally stable, and it could effectively replace synthetic plastic packaging. The interaction of fibroblast and MDA breast cancer cells with the dialyzed and diafiltered keratin films were examined with unexpected outcomes; both cell lines attached, proliferated and spread well with an elongated morphology on the dialyzed keratin substrate. On the other hand, these cells did not spread on the diafiltered keratin film and remained with round morphology. Some toxicity was detected for diafiltered keratin film, but it was unlikely that there were still traces of chemicals—used for extraction—to cause this toxicity. This unexpected observation might be caused by the smooth surface of diafiltered keratin film, which had no porosity. Moreover, it was hypothesized that removing some amino acids in low molecular weight polypeptides could affect cell binding and spreading on these films. This hypothesis should be further investigated. Based on these observations, diafiltered keratin films—unlike their predecessors—were not suitable for cell related applications; however, their enhanced ductility could make them potentially useful candidates for a new generation of environmental friendly packaging materials.

**Acknowledgments:** Authors would like to thank University of Melbourne and Australian research council (ARC) for providing the fund for this research.

**Author Contributions:** Elham Bidram carried out the cell experiment section (30%). Halleh Atri carried out the rest of the study (70%). The study was conducted under the supervision of David E. Dunstan.

**Conflicts of Interest:** The authors declare no conflict of interest.

## References

- Poole, A.J.; Church, J.S.; Huson, M.G. Environmentally sustainable fibers from regenerated protein. *Biomacromolecules* **2008**, *10*, 1–8. [[CrossRef](#)] [[PubMed](#)]
- Ottoman, J.A.; Stafford, E.R.; Hartman, C.L. Avoiding green marketing myopia: Ways to improve consumer appeal for environmentally preferable products. *Environ. Sci. Policy Sustain. Dev.* **2006**, *48*, 22–36. [[CrossRef](#)]
- Mohanty, A.K.; Misra, M.; Drzal, L.T. Sustainable bio-composites from renewable resources: Opportunities and challenges in the green materials world. *J. Polym. Environ.* **2002**, *10*, 19–26. [[CrossRef](#)]
- Guille, M.M.G.; Mosser, G.; Helary, C.; Eglin, D. Bone matrix like assemblies of collagen: From liquid crystals to gels and biomimetic materials. *Micron* **2005**, *36*, 602–608. [[CrossRef](#)] [[PubMed](#)]
- Keogh, J.R.; Eaton, J.W. Albumin binding surfaces for biomaterials. *J. Lab. Clin. Med.* **1994**, *124*, 537–545. [[PubMed](#)]
- Sivakumar, M.; Rao, K.P. Preparation, characterization and *in vitro* release of gentamicin from coralline hydroxyapatite–gelatin composite microspheres. *Biomaterials* **2002**, *23*, 3175–3181. [[CrossRef](#)]
- Kang, H.W.; Tabata, Y.; Ikada, Y. Fabrication of porous gelatin scaffolds for tissue engineering. *Biomaterials* **1999**, *20*, 1339–1344. [[CrossRef](#)]
- Rockwood, D.N.; Preda, R.C.; Yucel, T.; Wang, X.; Lovett, M.L.; Kaplan, D.L. Materials fabrication from *Bombyx mori* silk fibroin. *Nat. Protoc.* **2011**, *6*, 1612–1631. [[CrossRef](#)] [[PubMed](#)]
- Omenetto, F.G.; Kaplan, D. A new route for silk. *Nat. Photonics* **2008**, *2*, 641–643. [[CrossRef](#)]
- Rouse, J.G.; van Dyke, M.E. A review of keratin-based biomaterials for biomedical applications. *Materials* **2010**, *3*, 999–1014. [[CrossRef](#)]
- Aluigi, A.; Vineis, C.; Ceria, A.; Tonin, C. Composite biomaterials from fiber wastes: Characterization of wool–cellulose acetate blends. *Compos. Part A Appl. Sci. Manuf.* **2008**, *39*, 126–132. [[CrossRef](#)]
- Reichl, S.; Borrelli, M.; Geerling, G. Keratin films for ocular surface reconstruction. *Biomaterials* **2011**, *32*, 3375–3386. [[CrossRef](#)] [[PubMed](#)]

13. Scheibel, T. Protein fibers as performance proteins: New technologies and applications. *Curr. Opin. Biotech.* **2005**, *16*, 427–433. [[CrossRef](#)] [[PubMed](#)]
14. Strelkov, S.V.; Herrmann, H.; Aebi, U. Molecular architecture of intermediate filaments. *Bioassays* **2003**, *25*, 243–251. [[CrossRef](#)] [[PubMed](#)]
15. Salminen, E.; Rintala, J. Anaerobic digestion of organic solid poultry slaughterhouse waste—A review. *Bioresour. Technol.* **2002**, *83*, 13–26. [[CrossRef](#)]
16. Schrooyen, P.M.M.; Dijkstra, P.J.; Oberthür, R.C.; Bantjes, A.; Feijen, J. Stabilization of solutions of feather keratins by sodium dodecyl sulfate. *J. Colloid. Interf. Sci.* **2001**, *240*, 30–39. [[CrossRef](#)] [[PubMed](#)]
17. Onifade, A.A.; Al-Sane, N.A.; Al-Musallam, A.A.; Al-Zarban, A. A review: Potentials for biotechnological applications of keratin-degrading microorganisms and their enzymes for nutritional improvement of feathers and other keratins as livestock feed resources. *Bioresour. Technol.* **1998**, *66*, 1–11. [[CrossRef](#)]
18. European Man Made Fiber Association. Available online: <http://www.cirfs.org> (accessed on 29 October 2015).
19. Hearle, J.W.S.; Woodings, C. Fibers Related to Cellulose. In *Regenerated Cellulose Fibers*; Woodhead Publishing: Sawston, Cambridge, UK, 2001; pp. 156–173.
20. Ministry of Textiles. Available online: [http://www.texmin.nic.in/policy/Fibre\\_Policy\\_Sub\\_%20Groups](http://www.texmin.nic.in/policy/Fibre_Policy_Sub_%20Groups) (accessed on 26 October 2015).
21. Langer, R.; Tirrell, D.A. Designing materials for biology and medicine. *Nature* **2004**, *428*, 487–492. [[CrossRef](#)] [[PubMed](#)]
22. Padgett, T.; Han, I.; Dawson, P. Incorporation of food-grade antimicrobial compounds into biodegradable packaging films. *J. Food Prot.* **1998**, *61*, 1330–1335. [[PubMed](#)]
23. Zahn, H.; Föhles, J.; Nlenhaus, M.; Schwan, A.; Spel, M. Wool as a biological composite structure. *Ind. Eng. Chem. Prod. Res. Dev.* **1980**, *19*, 496–501. [[CrossRef](#)]
24. Fudge, D.S.; Gardner, K.H.; Forsyth, V.T.; Riekel, C.; Gosline, J.M. The mechanical properties of hydrated intermediate filaments: Insights from hagfish slime threads. *Biophys. J.* **2003**, *85*, 2015–2027. [[CrossRef](#)]
25. Bertaude, J.; Qin, Z.; Buehler, M.J. Intermediate filament-deficient cells are mechanically softer at large deformation: A multi-scale simulation study. *Acta Biomater.* **2010**, *6*, 2457–2466. [[CrossRef](#)] [[PubMed](#)]
26. Thompson, E.; O'donnell, I. Studies on oxidised wool. I. A comparison of the completeness of oxidation with peracetic and performic acid. *Aust. J. Biol. Sci.* **1959**, *12*, 282–293.
27. McHugh, T.H.; Weller, C.L.; Krochta, J.M. *Edible Coatings and Films to Improve Food Quality*; CRC Press: Boca Raton, FL, USA, 1994.
28. Krochta, J.M. Proteins as Raw Materials for Films and Coatings. In *Protein-Based Films and Coatings*; Gennadios, A., Ed.; CRC Press: Boca Raton, FL, USA, 2001; pp. 1–41.
29. Tachibana, A.; Furuta, Y.; Takeshima, H.; Tanabe, T.; Yamauchi, K. Fabrication of wool keratin sponge scaffolds for long-term cell cultivation. *J. Biotech.* **2002**, *93*, 165–170. [[CrossRef](#)]
30. Katoh, K.; Tanabe, T.; Yamauchi, K. Novel approach to fabricate keratin sponge scaffolds with controlled pore size and porosity. *Biomaterials* **2004**, *25*, 4255–4262. [[CrossRef](#)] [[PubMed](#)]
31. Hamasaki, S.; Tachibana, A.; Tada, D.; Yamauchi, K.; Tanabe, T. Fabrication of highly porous keratin sponges by freeze-drying in the presence of calcium alginate beads. *Mater. Sci. Eng. C* **2008**, *28*, 1250–1254. [[CrossRef](#)]
32. Aluigi, A.; Varesano, A.; Montarsolo, A.; Vineis, C.; Ferrero, F.; Mazzuchetti, G.; Tonin, C. Electrospinning of keratin/poly (ethylene oxide) blend nanofibers. *J. Appl. Polym. Sci.* **2007**, *104*, 863–870. [[CrossRef](#)]
33. Zoccola, M.; Aluigi, A.; Vineis, C.; Tonin, C.; Ferrero, F.; Piacentino, M.G. Study on cast membranes and electrospun nanofibers made from keratin/fibroin blends. *Biomacromolecules* **2008**, *9*, 2819–2825. [[CrossRef](#)] [[PubMed](#)]
34. Yamauchi, K.; Yamauchi, A.; Kusunoki, T.; Kohda, A.; Konishi, Y. Preparation of stable aqueous solution of keratins, and physicochemical and biodegradational properties of films. *J. Biomed. Mater. Res.* **1998**, *31*, 439–444. [[CrossRef](#)]
35. Katoh, K.; Shibayama, M.; Tanabe, T.; Yamauchi, K. Preparation and physicochemical properties of compression-molded keratin films. *Biomaterials* **2004**, *25*, 2265–2272. [[CrossRef](#)] [[PubMed](#)]
36. Howie, A.; Brewer, D.B.; Howell, D.; Jones, A.P. Physical basis of colors seen in Congo red-stained amyloid in polarized light. *Lab. Invest.* **2008**, *88*, 232–242. [[CrossRef](#)] [[PubMed](#)]

37. Aluigi, A.; Vineis, C.; Varesano, A.; Mazzuchetti, G.; Ferrero, F.; Tonin, C. Structure and properties of keratin/PEO blend nanofibers. *Euro. Pol. J.* **2008**, *44*, 2465–2475. [[CrossRef](#)]
38. Tanabe, T.; Okitsu, N.; Tachibana, A.; Yamauchi, K. Preparation and characterization of keratin–chitosan composite film. *Biomaterials* **2002**, *23*, 817–825. [[CrossRef](#)]
39. Lowry, O.H.; Rosebrough, N.J.; Farr, A.L.; Randall, R.J. Protein measurement with the Folin phenol reagent. *J. Boil. Chem.* **1951**, *193*, 265–275.
40. Ellman, G.L. Tissue sulfhydryl groups. *Arch. Biochem. Biophys.* **1959**, *82*, 70–77. [[CrossRef](#)]
41. Laemmli, U.K. Cleavage of structural proteins during the assembly of the head of bacteriophage T4. *Nature* **1970**, *227*, 680–685. [[CrossRef](#)] [[PubMed](#)]



© 2015 by the authors; licensee MDPI, Basel, Switzerland. This article is an open access article distributed under the terms and conditions of the Creative Commons by Attribution (CC-BY) license (<http://creativecommons.org/licenses/by/4.0/>).